Beam-Column Analysis

Effects of residual stresses and geometric imperfections

Pedro Melo
pedro.melo@tecnico.ulisboa.pt

Instituto Superior Técnico, Lisboa, Portugal

July 2016

Abstract

A numerical model is developed towards the production of geometric nonlinear analysis of steel structures, namely columns and beam-columns. The model executes second order analysis, taking into account geometrical and material nonlinearities. As initial conditions the model considers both geometrical and structural imperfections.Numerically the model consists on an application of a distributed-plasticity *Euler-Bernoulli* beam displacement-based finite element method and of a Newton-Raphson nonlinear equation resolution algorithm. The developed model was validated by comparing its solutions with the ones presented in a PhD dissertation by Ofner (1997), which was obtained through the use of the automatic computation software *Abaqus* and was used as basis for the calibration of both methods available in the EN1993-1-1:2005 for the calculation of the interaction factors involved in the buckling ultimate limit state safety verification of beam-columns. The developed model is then employed to evaluate the applicability of these same two methods, relying on an extensive set of simulations.

Moreover, the model is also applied to study the effect of varying the direction of the geometrical imperfection relative to the location of the weld, i.e. relative to the orientation of the residual stress field, in what concerns the behaviour of cold formed circular tubes with a single longitudinal weld.
Keywords: steel structures, finite element method, residual stresses, second order analyses, geometrically nonlinear, physically nonlinear.

1. Introduction

Stability has almost three centuries of history already, starting with the *Euler* formula in the year 1744. This formula defined the buckling load of a column, depending on its length and cross-section shape. *Lagrange* introduced the concept of buckling mode and *Lamarle* defined the stress associated with the phenomenon. *Jasinsky* introduced the concept of buckling length, which allowed for the extension of the application of *Euler* and *Lamarle* formulas to elements with other support conditions.

Navier was one of the first to point out that the results provided by the above mentioned formulas represented an upper-bound to the ultimate resistances found in real columns. It was noted that the buckling resistance of columns is strongly influenced by its imperfections. In 1807, *Young* in addition to introducing the concept of modulus of elasticity also presented the solution for the displacements of a simply-supported column with a geometrical imperfection with the shape of a half-sine wave.

In 1886, *Ayrton* and *Perry*, considering a imperfection shape for the simply-supported column as a combination of the buckling modes, i.e. a Fourier series of sines, defined a criterion for the column resistance. The criterion was the yielding of the most compressed fiber of an axially compressed column with an imperfection defined through an adimensional factor.

In 1925, *Robertson*, after a set of experimental measurements, suggested that the adimensional imperfection factor would be accurately given by $\theta = 0.003\lambda$. With this formula *Robertson* introduced the concept of equivalent geometric imperfection, an imperfection deliberately overestimated, with the purpose of taking into account other imperfections which are not as easy to simulate. Also worth of mention is the fact that the Robertson formula makes the magnitude of the imperfection dependent on the type of cross-section, (Maquoi, 1980).

In 1955, the *European Convention for Constructional Steelwork* ("ECCS") was established with the objective of standardising the design methods of steel construction in Europe. With the creation of the European Community starts the project for

the definition of the European structural norms, the "Eurocodes", being the EN1993 ("EC3") related to the safety verification of steel construction.

In the sixties, the eighth technical committee ("TC8") of the ECCS (Stability Problems) produces a vast campaign of column tests, more than a thousand experiments over seven European countries, together with the numerical simulation and analytical study of the problem. As a result, in 1970, the technical committee proposed three design curves (a, b and c).

In 1976, *Young* and his team proposed the introduction of a plateau for extremely small slendernesses in the column design curves, in order to take into account the strain-hardening which had not been included in the numerical models. Together with this alteration of the shape of the column curves, two new curves were introduced: a less severe one for high strength steel (a_0) and a fifth curve, the most severe, for cross-sections with high thicknesses (d).

In 1979, *Maquoi* and *Rondal* proposed the formulation for the "European column design curves", based on the *Ayrton-Perry* formula, which is still in use today. This formulation consists on assigning to the adimensional imperfection factor the following formula: $\theta = \alpha(\bar{\lambda} - 0.2)$, being "$\alpha$" an imperfection parameter, calibrated so the results from the *Ayrton-Perry* formula would present a good agreement with the results of the simulations. Taking into account residual stresses, an yield limit is no longer reasonable, thus the result of a simulation is considered reached when no further equilibrium position can be found.

The European column design curves were defined based on the specific case of a simply-supported column in a steel grade $S235$, with an initial geometric imperfection with the shape of a half-sine wave with the amplitude of $L/1000$. This imperfection was estimated in order to take into account also the other member geometric imperfections. This value was already chosen by *Jasinsky* as a realistic approximation of the imperfections found in construction sites. The curves can then be extrapolated for other support conditions and steel grades.

The first version of "EC3" was published in 1984. In 1992, the European Committee for Standardization ("CEN") publishes a new version of EC3 with European pre-norm status, (ENV1993-1-1:1992), and in 2005, the present version as European norm, (EN1993-1-1:2005).

Regarding the column formulation in "EC3", it is important to note that it is independent from the steel grade, which implies that the initial equivalent geometric imperfection is proportional to the resistance of the material, for which there is no justification, (Dwight, 1975). In fact, experimental results show that with increasing material resistance the reduction of resistance due to imperfections decreases. However, the diagrams of residual stresses presented in ECCS(1976), used in the column curve simulations, create a correspondence between the magnitude of the residual stresses and the yield stress of the structural element material. No such correspondence can be identified from the experimental measurements in the literature.

As for the beam-column elements, the method available in the ENV1993-1-1:1992 for the definition of the interaction factors to be adopted for the buckling safety verification of these elements, had some physical inconsistences and was excessively conservative, (Greiner, 2006). For these reasons, "TC8" carried out an extensive numerical simulation study (Ofner, 1997) with which, along with a group of experimental results, new methods would be calibrated. Two methods have resulted from that initiative: one from an Austrian-Germanic origin, more practical for hand calculations and one with a Belgian-Franc origin, more theoretically transparent. These are the methods currently adopted in the EN1993-1-1:2005.

A numerical model was developed in *Matlab* environment capable of studying the details just described in the stability problem.

In this paper the developed model was applied with the purpose of evaluating the results of applying the two new methods for the calculation of the interaction factors. A brief evaluation of the impact of modifying the intensity of the residual stresses in hot-rolled cross-sections was performed as well.

The model was also adopted to evaluate the impact of varying the direction of the initial geometrical imperfection, with respect to the position of the weld, in what concerns the behaviour of cold-formed circular hollow sections with a single longitudinal weld.

2. Implementation

The developed numerical model consists on a displacement-based *Euler-Bernoulli* beam finite element model. The model performs second-order analysis including both geometrical and material nonlinearities. With that purpose, the transverse displacement field is approximated using cubic *Hermitian* polynomials while for the axial displacements the linear *Lagrangian* polynomials are used, resulting in a six degree-of-freedom finite element. Therefore, the geometric component of the nonlinear stiffness matrix is uncoupled from the elastic one.

As for material nonlinearities, a distributed-plasticity (plastic-zone) approach is used, aiming for a more accurate simulation of the spread of

plasticity over the section and along the element. Additionally, these approaches represent the most generic and precise manner to introduce residual stresses in the analysis. For integration purposes, the finite elements are subdivided into cross-sections, at the integration points, which are further subdivided. A stress control has to be kept for each fibre at each cross-section because after yielding a fiber no longer contributes for the stiffnesses of the corresponding cross-sections, which have to be integrated and updated. The initial values of the stress registry simply correspond to the diagram of residual stresses. This methodology, though much heavier in computational terms, is simpler and more precise than the alternatives.

Since the analysis to be performed are nonlinear in nature, the usual linear procedure associated with displacement-based finite element methods will not work. For dealing with the nonlinear aspect of the problem, the *Newton-Raphson* algorithm was adapted to find the load bearing capacity of the structural elements. This algorithm is an incremental iterative procedure, the most traditional and most simple to understand and to implement from the available ones, with load increments in which the tangent stiffness matrix is updated at the beginning of each iteration and increment.

Regarding the numerical integration process, a variation of the *Gauss-Legendre* quadrature is used, the *Gauss-Lobatto* one. The advantage of the *Gauss-Lobatto* quadrature is the imposition that two of the integration point are located exactly at the extremities of the domain, despite the number of integration points being adopted. Since plasticity tends to concentrate at the extremities of the elements and start at the tips of the cross-sections, this choice of alternate quadrature allows a more precise monitoring of the spread of plasticity. On the other hand the abscissa of two of the integration points are pre-established, it is then generally necessary one more point in this quadrature, compared to the number of points needed in the standard one, to integrate exactly the same polynomial.

The developed numerical model is written in *Matlab* environment, being prepared to obtain input from an *Excel* file; the residual stresses diagrams for hot-rolled I/H sections and rectangular hollow sections, and cold-formed circular hollow sections are already built-in. The developed model is also capable to distinguish two different components of loading, a uniform one and a incremental one.

Given the volume of results planned to be obtained, the process of acquiring them is automatic, pre-establishing the simulations to be run, having the program alter the input itself and record the result in an appropriate manner.

3. Validation and Application

3.1. Validation

The developed numerical model ("DNM") is validated comparing its solutions with the results presented by Ofner (1997). These results were chosen for validation, not only because of their quantity and quality, but also because these results were adopted for the calibration of both methods available in the EN1993-1-1:2005 for the verification of beam-column buckling. In fact Ofner, performed more than 20000 second-order geometrically and materially non-linear simulations of steel members, taking into account initial residual stresses, through a user-defined subroutine introduced in the Abaqus software, and geometrical imperfections.

Ofner simulated simply-supported steel members with four different sections — $IPE200$, $IPE500$, $HEB300$, $RHS200 \times 100 \times 10$ — in steel of grade $S235$. For the analysis on the plane, Ofner presents analysis for both principal planes for members with three different values of normalized slenderness — $0,5$ $1,0$ $1,5$ — under six different transverse load configurations:

A two equal concentrated moments on the beam ends, making a uniform moment diagram;

B a single concentrated moment on an extremity, making a linear moment diagram with zero on one extremity;

C two symmetrical concentrated moments on the extremities, making a linear moment diagram;

D concentrated load at mid-span;

E constant distributed load;

F combination of configurations "A" and "D", making a bilinear moment diagram where the mid-span value is symmetrical with the ones at the extremities.

In these plane analysis the geometrical imperfections implemented have the form of a half-sine wave with an amplitude of $L/1000$. Regarding the residual stresses diagrams, the widely accepted ones from the ECCS(1976), used in the definition of the European column curves, were applied.

The results in Ofner (1997) are presented in graphics and the curves of the graphics corresponding to plane analysis were reproduced with eight simulations in the developed model, making a subtotal of approximately 1150 simulations. The results regarding buckling along the strong axes of an IPE200 from both models are presented in figure 1 the remaining in Melo (2016). As can be seen in these figures, and in the ones in the reference, the results from the developed model show an excellent

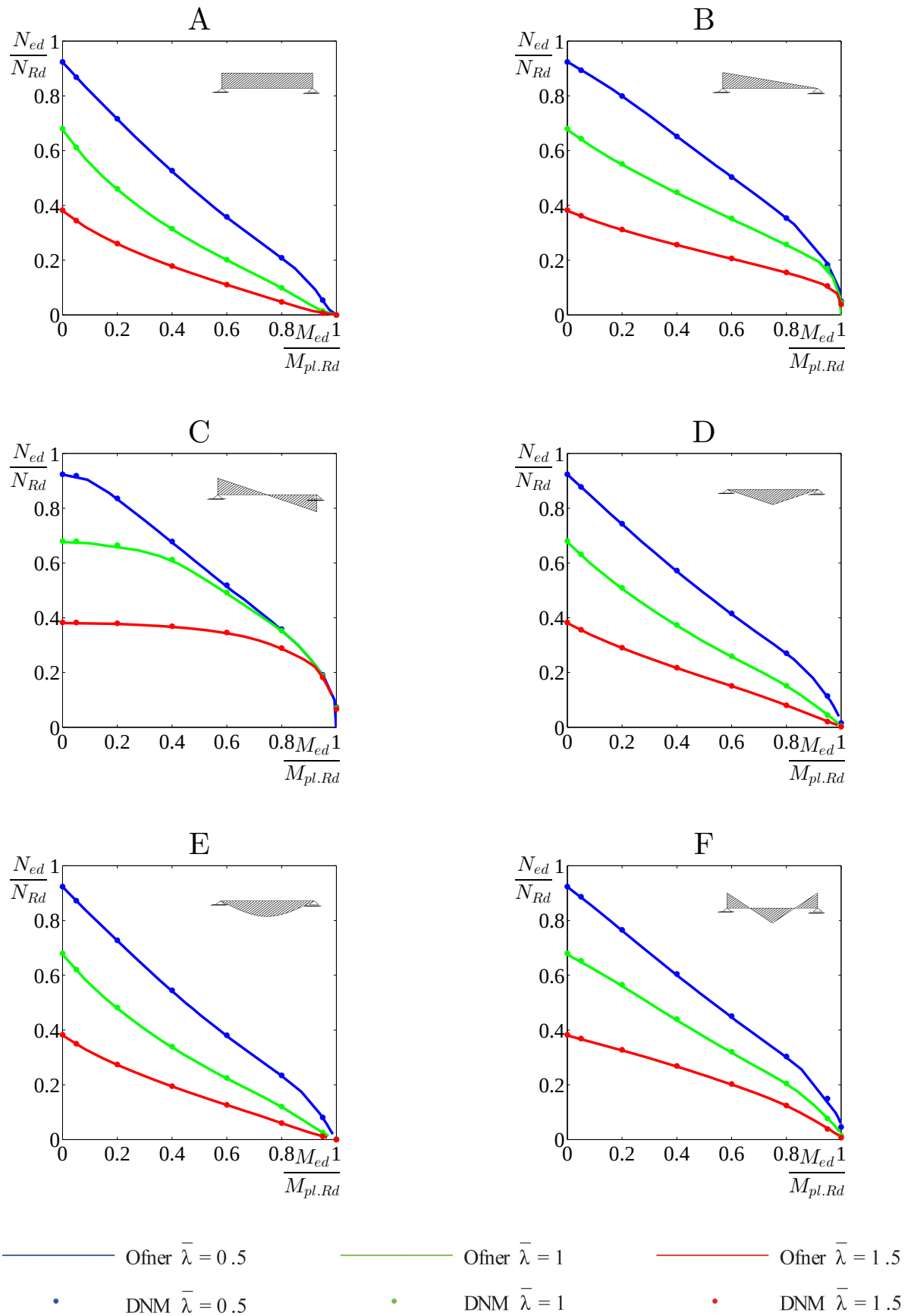

Figure 1: IPE200 strong axes buckling DNM vs. Ofner

	Strong axes			Weak axes		
	Average	Maximum		Average	Maximum	
		Non-conservative	Conservative		Non-conservative	Conservative
Method 1	4,8%	5,3%	14,9%	4,5%	5,3%	19,7%
Method 2	5,1%	5,3%	26,0%	9,1%	5,3%	28,2%

Table 1: Whole results.

agreement with the results by Ofner (1997). Therefore the developed numerical model is considered validated.

3.2. Results

The developed numerical model is adopted to evaluate the applicability of the two methods in the EN1993-1-1:2005 regarding the verification of beam-column buckling, namely: method 1, presented in annex "A" and described in Boissonnade(2004) and method 2, presented in annex "B" and explained in Greiner(2006). The model was also applied to study the impact of varying the direction of the initial geometrical imperfection, with respect to the position of the fillet weld in the behaviour of cold-formed circular hollow sections with a single longitudinal weld.

3.2.1 Results hot-rolled

Firstly, the set of gathered results is expanded to HEA sections, since these are the sections better designed to be used as columns. The analysed sections are a $HEA200$ in $S235$ steel and a $HEA500$ in $S355$, these were simulated for buckling about both principal axis, as were the other sections, with the same three values of normalized slenderness ($0,5$ $1,0$ $1,5$), under the same six different transverse load configurations, described in the previous section, with the same initial conditions. The set of results now amounts to more than 1700 simulations, which cannot all be reproduced in this document. The results for both axes of the IPE200 section are displayed in figures 2 and 3, along with the results obtained from both methods available in EN1993-1-1:2005. The remaining results are available in Melo (2016), in the same format.

Considering the examples analysed (e.g. figures 2 and 3), one can safely say that, for I/H type sections, method 2 is the most conservative of the two, when analysing buckling about the weaker axes. As for the strong axis it is not possible to determine which of the two methods is more conservative. This is because the result from method 2 gives a clearly better approximation for buckling about the strong axes than along the weak axes.

Regarding the differences in behaviour under the six transverse load configurations, it is possible to notice that the quality and consistency of the answer of both methods, when analysing buckling about the strong axis, gradually worsens from configuration "A" to "C", i.e. worsens with the progressive inversion of the concentrated moments at the beam ends. Under configuration "A" the quality of the answers is approximately constant and independent of both method and slenderness, while under configuration "C" the quality of the answer varies with the intensity of the transverse load, and it is also no longer independent with respect to the slenderness and method chosen. Similarly, under configurations "D" and "E" the answer behaves as under configuration "A", and under configuration "F" behaves as under configuration "C", i.e. while there is only transverse loads the methods have a good behaviour, when there is a combination of transverse loads and concentrated end moments the behaviour of the answers is not as good.

Regarding buckling about the weak axis, for I/H type sections, no distinction can be made between the behaviour under the different transverse load configurations, all six of them being most similar to the behaviour under configuration "C" about the strong axis.

Also relevant to note that for all analysed sections the case where method 2 is most conservative is for the element with normalized slenderness of $1,5$ and a transverse load configuration "C", about the strong axis this is an isolated case while about the weak axis there are other close simulations. Such conservative results are partly due to the purposefully conservative lower limit introduced in the *Austin* formula ($0.6+0.4\psi \geq 0.4$), which is used for the calculation of the equivalent uniform moment factor in method 2.

Specifically for the $RHS200 \times 100 \times 10$ section, as expected, it features a lower level of distinction between the performance about the two axes, and the results obtained for this section are most similar with the ones from the I/H type sections about the strong axis, particularly in what concerns the behaviour under the different transverse load configurations. Hence, method 2 no longer exhibits such a higher level of conservatism about the weaker axis in comparison with method 1.

An analysis of the whole results, evaluating the error of the obtained solution relatively to both methods, is summarized in table 1. The results found for method 1 are in accordance with the ones reported by Boissonnade(2004) and clearly more satisfactory than the ones presented in the

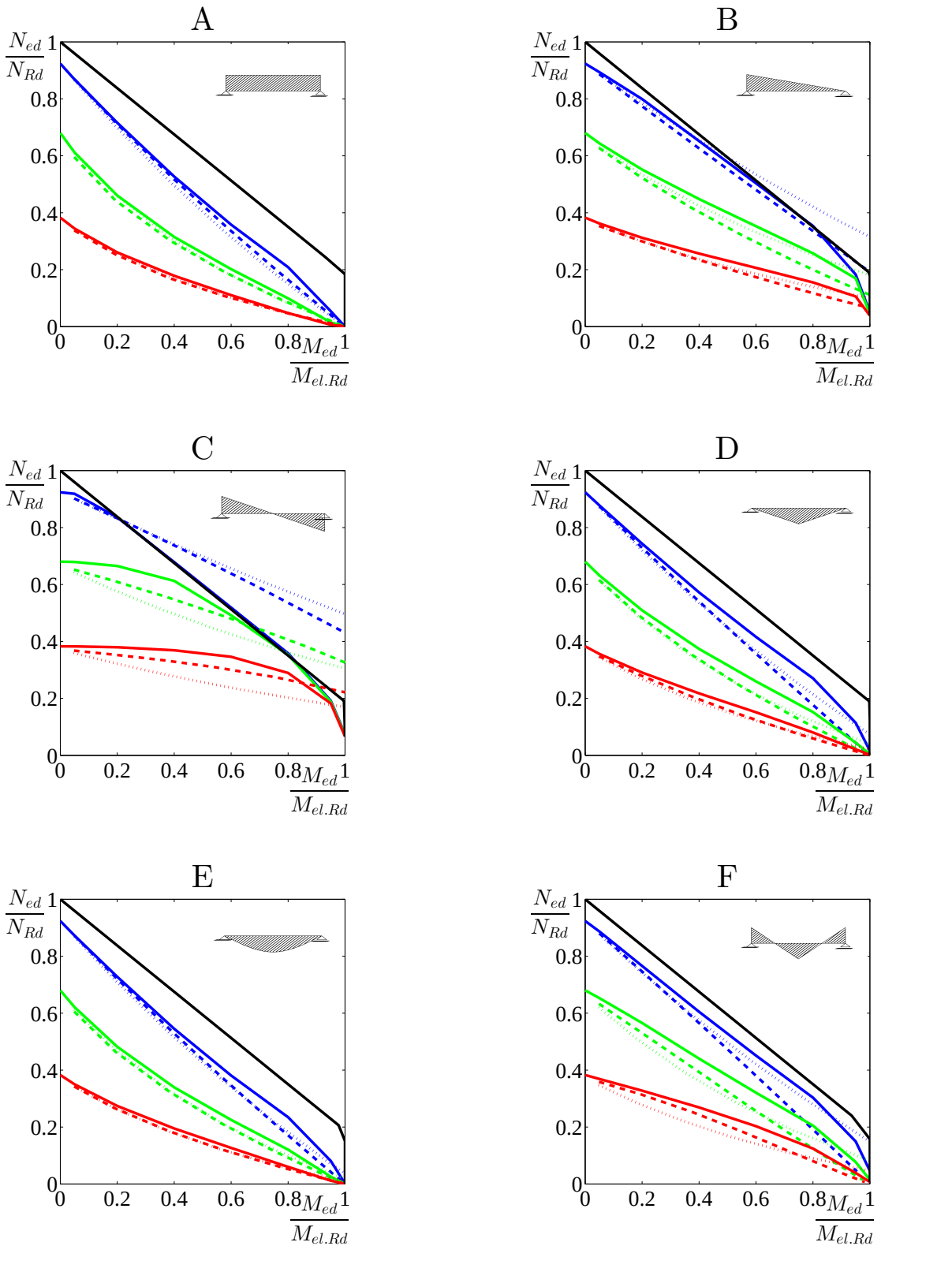

Figure 2: IPE200 strong axes buckling DNM vs. EC3

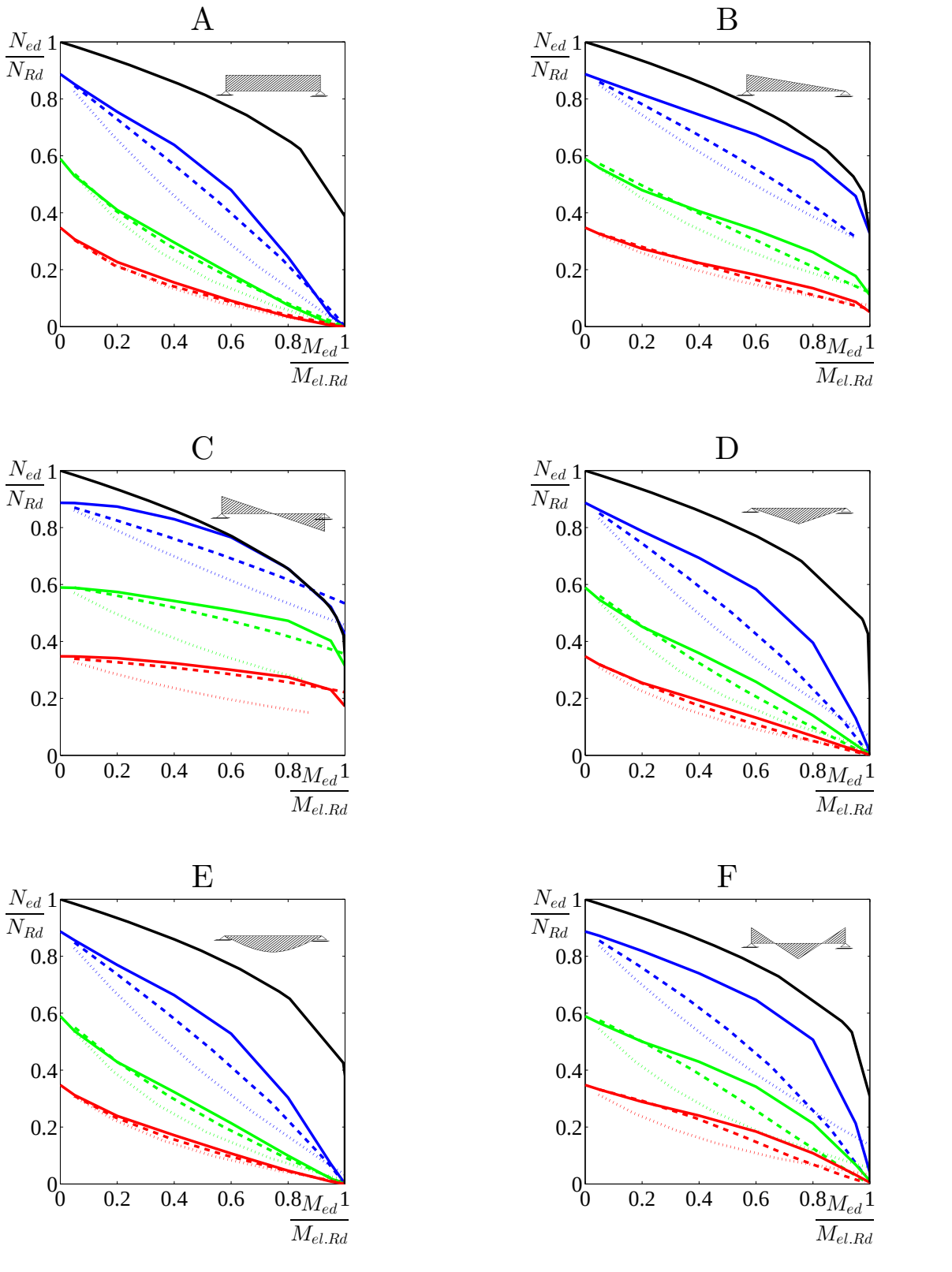

Figure 3: IPE200 weak axes buckling DNM vs. EC3

same document for the previous version of EC3, ENV1993-1-1:1992, — average error $24,4\%$, maximum conservative error $87,0\%$. The presented numbers imply that the errors are bigger about the weak axis and using method 2, however, it is important to underscore that the set of results obtained is limited to plane analysis and these methods have a domain which includes spatial problems with possibility of lateral-torsional buckling.

Furthermore, a brief analysis is made about the influence of the magnitude of the residual stresses on the ultimate resistance of the steel elements. In theoretical terms as well as in experimental measurements, the intensity of the residual stresses does not depend on the steel grade. However, the widely used formulas presented in ECCS(1976) establish a relation between the intensity of the residual stresses and the yield stress of the steel used. With this objective the beam-column results of the $HEA500$ in $S355$ are repeated, but with the residual stresses scaled as considering the element made of $S235$ steel. In addition, a series of columns are simulated with several values of slenderness and with both magnitudes of residual stresses, analysed about both principal inertia axes.

It was found that by introducing residual stresses proportional to $S235$ in an $S355$ steel element, one obtains a slightly higher ultimate resistance: maximum of $3,5\%$ in columns (essentially in the weak axes for normalized slenderness close to 1), and 5% in beam-columns (concentrated in the weak axes in the area with transversal loads with lower intensity). The significative difference between the reduction in the intensity of residual stresses and the gain in resistance comes from the fact that, although the reduction in residual stresses increases the elastic load bearing capacity of the element, it also reduces the difference between the elastic and inelastic load bearing capacities.

3.2.2 Results CHS

The model was also adopted for the analysis of columns with a CHS section. The effect of varying the direction of the geometrical imperfection, relatively to the location of the weld, with respect to the behaviour of cold formed circular tubes with a single longitudinal weld was analysed.

Since there is no standard residual stresses diagram for cold-formed circular hollow sections ("CHS"), a diagram was defined by considering that the components of residual stresses due to the production process of the original steel plate and bending in the circular shape are negligible when compared with the component due to the welding. In so being, the applied residual stresses diagram is derived from the formula presented in ECCS(1976) for the residual stresses diagram of a plate with a single weld at one edge. the formula is adapted for a half-circumference, being written as:

$$\sigma_c = f_y \times \frac{2\left(\cos\left(\psi\right)+1\right)\psi + \sin\left(\psi\right)\left(\pi-\psi\right)^2}{2\left(\cos\left(\psi\right)+1\right)\left(\pi-\psi\right) - \sin\left(\psi\right)\left(\pi-\psi\right)^2}; \tag{1}$$

$$\sigma_t = \sigma_c - 2f_y \times \frac{\psi}{\pi-\psi}; \qquad \psi = \pi \times \frac{c \times b}{2}; \tag{2}$$

where "c" is the width of the tension block at each side of the weld, given by:

$$c = \frac{12000 \times p \times A_w}{f_y \times \sum t} \qquad (mm)\,, \tag{3}$$

where "p" is the process efficiency factor, assumed $0,9$ for submerged arc; "A_w" is the cross-section area of added weld metal in mm^2; "$\sum t$" is the sum of the plate thickness at the weld in mm and "b" is the perimeter in mm. In addition, the yield stress should be introduced in MPa. The resulting diagram is presented in figure 4, linear with respect to the centre angle.

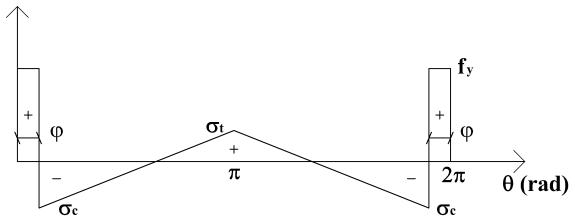

Figure 4: Residual stresses diagram in a circular hollow section due to a single weld.

In what concerns the residual stresses in this type of section it is only left to specify how "A_w" is obtained. For a single curve — curve c — to be able to suitably adapt to all cold-formed circular hollow sections the same geometrical layout for the fillet weld must be applicable to all sections. The layout applied in this study is the one illustrated in figure 5.

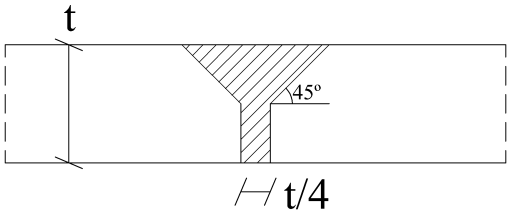

Figure 5: Geometrical layout for the weld cross-section.

The studied section is a $CHS457 \times 8$ in $S235$ steel grade, of resistance class 2 and to which correspond the following data for the definition of the residual stresses diagram:

$\psi = 0,41rad; \quad \sigma_c = 142,2MPa; \quad \sigma_t = 71,768MPa.$

Three combinations of imperfections are studied. Combination "A" considers the residual stresses and the initial geometric imperfection in opposite directions by placing the fillet weld at the inner side of the initial curvature, illustrated in figure 6a. Combination "B" considers both imperfections in orthogonal directions, by placing the fillet weld at 90º with the initial geometrical imperfection, represented in figure 6b. Combination "C" is the opposite of combination "A", both imperfections have the same direction placing the fillet weld at the outer side of the initial curvature, presented in figure 6c. Also illustrated on figures 6 is a qualitative stress diagram due to loading and element geometry, termed "σ_{carreg}".

Combination "A" is instinctively more constraining since it overlaps the area on the residual stresses diagram with the higher intensities, both in compression and in tension, with the area most compressed in "σ_{carreg}". Consequently, reduces both the elastic and inelastic load bearing capacities. By opposition, combination "C" is instinctively the least constraining as it overlaps the area on the residual stresses diagram with the higher intensities with the area least compressed in "σ_{carreg}". In what concerns combination of imperfections "B", although it overlaps the area on the residual stresses diagram with the higher intensities with the area with mean compression in "σ_{carreg}", it concentrates the tensioned areas of the residual stresses diagram around the centre of gravity of the section. In this way, as the compressed areas are the first to yield, the section rapidly loses the greater part of its bending moment resistance. For this reason, for small values of slenderness this second combination of imperfections yields lower values of ultimate element resistance than combination "A".

It is important to note that the results obtained for combination "B" have an inherent error due to the fact that the column structural behaviour is biaxial bending as a result of the combination of imperfections considered. The developed numeric model only has the ability to analyse a single plane, the out-of-plane component is then neglected.

With respect to curve "c" ($\alpha = 0,49$), the column curve defined in EC3 for cold-formed hollow sections, the results attained with combination of imperfections "A" are in a good agreement: curve "c" is on the safe side throughout the slenderness range. As well as combination "B" for slendernesses greater than 1; for smaller slendernesses though, curve "c" is not on the safe side with respect to combination "B", the maximum non-conservative error found is 8%. As predicted, for slendernesses smaller than 2, combination "C" is not the constraining one, corresponding to values of ultimate resistance significantly greater than the other two

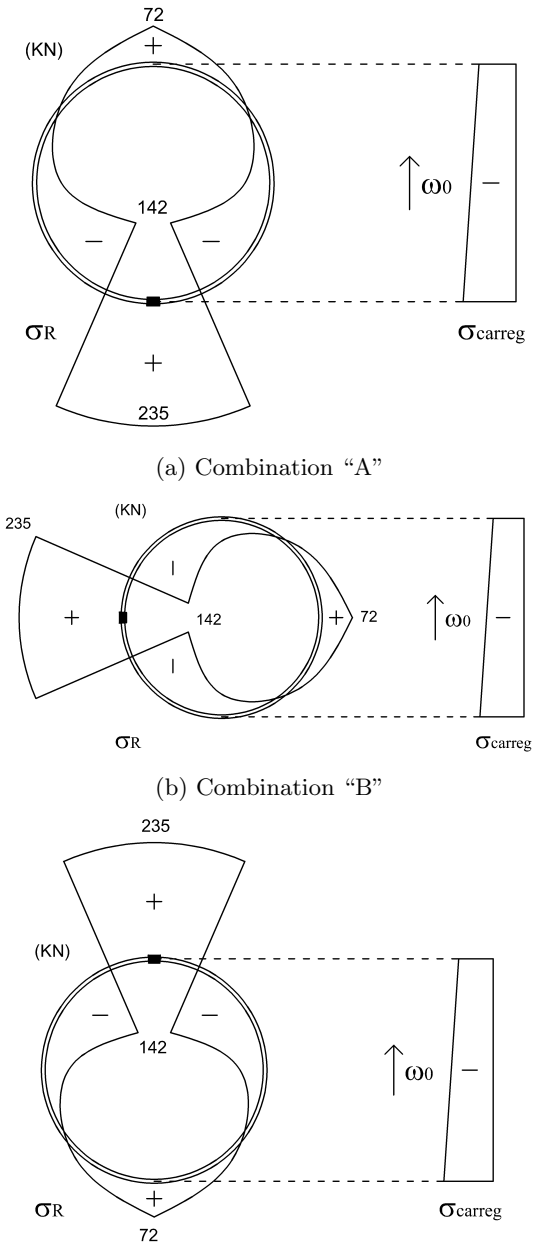

(a) Combination "A"

(b) Combination "B"

(c) Combination "C"

Figure 6: Qualitative diagrams of the residual stresses and stresses due to the loading and element geometry.

combinations. For values of slenderness greater than 2, combination "C" results in ultimate resistances lower than the ones obtained by the other two combinations and by curve "c", though with only slight differences.

The effect of the residual stresses in the deflections of the element, as obtained through the developed numeric model, is materialized through an additional bending moment in the inelastic sections. The stress diagram in a given section may be seen

Comprimento	L = 4m			L = 14m			L = 21m		
Combinação	A	B	C	A	B	C	A	B	C
Gomes (KN)	4231	3863	4306	2376	2105	2663	1325	1334	1542
DNM (KN)	4275	3974	4443	2416	2216	2704	1332	1399	1553
Erro	1,0%	2,9%	3,2%	1,7%	5,3%	1,5%	0,5%	4,9%	0,7%

Table 2: Agreement between the two models.

as the sum of the two components represented in figures 6. In the first stages of inelasticity one can consider that the component due to loading remains intact and that it is the residual stresses component which is "truncated". A truncated residual stresses diagram no longer possesses the auto-equilibrated characteristic, both in terms of axial force and moments, as illustrated in figure 7b.

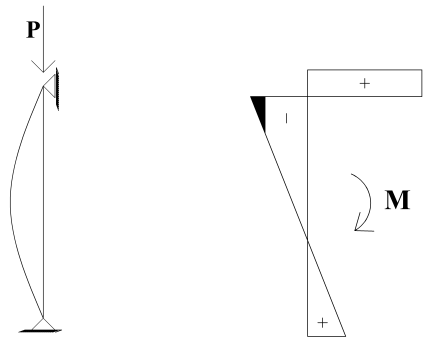

(a) (b)

Figure 7: (a) Imperfect column; (b) Qualitative diagram of truncated cross-sectional residual stresses, lateral view combination "C".

For small values of slenderness, in combination of imperfections "A" the moment from the truncated residual stresses is opposed to the one produced by the axial force, illustrated in figure 7a, therefore the need arises for bigger deflections in order to establish equilibrium. In combination "B" two moments arise from the truncated residual stresses: one has an effect similar to the one described for combination "A", the other one would give rise to out-of-plane deflections, thus bi-axial bending. In combination "C", once again, the effect is opposed to the one in combination "A", a moment arises with the same direction as the one produced by the axial force, making the equilibrium configuration less deformed.

As the effect of the geometric imperfection is proportional to the element slenderness and the effect of the residual stresses is not, for small values of slenderness, in combination "C" there must be a value of slenderness for which both effects balance each other out. In so being, along the results for this combination there are actually two different behaviours. For greater values of slenderness the effect from the geometric imperfection is predominant and the equilibrium path presents the expected form, progressive increase of the deflections as in the other combinations. For smaller values of slenderness there is a point along the equilibrium path in which the effects of the residual stresses overcome the effect of the geometrical imperfection arising a reduction or even inversion of the deflections.

The combination "C" becomes determining for slendernesses greater than 2, since for these values of slenderness, in terms of stresses, the effect of the moment produced by the axial force introduced surpasses its compressive effect and, in combination "C", the first areas to yield are no longer the compressive ones but the tensioned ones. This means that the moment due to the truncated residual stresses does not have the same direction as the one produced by the axial force anymore.

A comparison with the results obtained by Gomes (2014) was performed so as to evaluate the model accuracy. The results of Gomes are obtained through the use of shell elements in the computational software *Abaqus*. The section $CHS508 \times 8$ in $S355$ grade steel is the one chosen in the document, having the following data for the definition of the residual stresses diagram:

$$\psi = 0.49; \quad \sigma_c = 272MPa; \quad \sigma_t = 141MPa,$$

these possess some differences with the ones presented in Gomes (2014). The differences arise from practical considerations related with the dimensions of the shell elements and from the way by which the software produces the residual stresses. The values presented in the document are:

$$\psi = 0.47; \quad \sigma_c = 240MPa; \quad \sigma_t = 95MPa.$$

Three columns were simulated with the three different combinations of imperfections: $L = 21m$ $\bar{\lambda} \approx 1,7$; $L = 14m$ $\bar{\lambda} \approx 1,15$; $L = 4m$ $\bar{\lambda} \approx 0,33$. The results for these simulation are presented in table 2, both the ones from Gomes (2014) and the ones from the developed numerical model ("DNM"), as well as the error between the two models.

Taking into account that the *Abaqus* model is tri-dimensional and composed of shell elements, the

results obtained through the developed model are considered in satisfactory agreement. The greater error values found for combination "B" can be justified by the fact that the developed model neglects the out-of-plane deformations.

Finally, it is important to underscore that, to the best knowledge of the author, this is a subject not very well covered in the literature, and also that the residual stresses diagram, though similar to the one used by Gomes (2014) and to the one used in rectangular hollow sections, lacks experimental basis.

Additionally, the geometric layout used for the cross-section of the fillet weld may be a variable which influences the attained results and about which no study was performed.

4. Conclusions

An accurate and efficient numerical model capable of producing second-order analysis of steel members was successfully developed. The model consists on a distributed-plasticity *Euler-Bernoulli* beam displacement-based finite element model, resorting to the *Newton-Raphson* procedure to solve the non-linear component of the analysis. The results obtained with this model are generally in good agreement with the ones provided by the "EC3" formulations. Of particular note: the conservative results from method 2 for "I/H" type sections in buckling about the weak axes, specially when the end-moments are of opposite sign; and the non-conservative results in CHS cold-formed columns when the the fillet weld is positioned at a 90º angle with the geometrical imperfection direction.

Acknowledgements

I would like to express my sincere gratitude to my advisors Prof. Ricardo Vieira and Prof. Francisco Virtuoso for the continuous support of my study and knowledge. And I would like to thank my family for the support throughout writing this paper.

References

N. Boissonnade, J-P. Jaspart, J-P. Muzeau, and M. Villette. New interaction formulae for beam-columns in eurocode 3: The french–belgian approach. *Journal of Constructional Steel Research*, 60(3-5):421–431, 2004.

J.B. Dwight. Use of perry formula to represent the new european strut curves. *IABSE reports of the working commissions*, 23:399–412, 1975.

ECCS. Manual on stability of steel structures. *European Convention for Constructional Steelwork*, Publication 22, 1976.

EN1993-1-1:2005. Eurocode 3: Design of steel structures - Part 1-1: General rules and rules for buildings, CEN, Bruxelles, Belgium, May 2005.

ENV1993-1-1:1992. Eurocode 3: Design of steel structures - Part 1-1: General rules and rules for buildings, CEN, Bruxelles, Belgium, April 1992.

N. Gomes. Avaliação da contribuição das tensões residuais no comportamento estrutural de colunas e arcos tubulares. Master's thesis, Instituto Superior Técnico, Universidade Técnica de Lisboa, 2014.

R. Greiner and Lindner J. Interaction formulae for members subjected to bending and axial compression in eurocode 2 — the method 2 approach. *Journal of Constructional Steel Research*, 62(8): 757–770, 2006.

R Maquoi and J. Rondal. Le flambement des collones en acier. *Chambre Syndicale des Fabricants de Tubes d'Acier*, (notice 1091), 1980.

MathWorks Inc. Matlab, 2014.

P. Melo. Análise e dimensionamento de elementos estruturais em aço de alta resistência. Master's thesis, Instituto Superior Técnico, Universidade de Lisboa, 2016.

R. Ofner. *Traglasten von Stäben aus Stahl bei Druck und Biegung*. PhD thesis, Institut für Stahlbau, Holzbau und Flächentragwerke, Technische Universität Graz, Fakultät für Bauingenieurwesen, 1997.